A Novel Multimodal Collaborative-based Drone-assisted VANET Networking Model

Na Lin, Luwei Fu, Liang Zhao, *Member, IEEE*, Geyong Min, Ahmed Al-Dubai, *Senior Member, IEEE*, Haris Gacanin, *Senior Member, IEEE*

***Abstract*—Drones can be used in many assistance roles in complex communication situations and play key roles as aerial wireless relays to help terrestrial network communications. Although a great deal of emphasis has been placed on the drone-assisted networks, the majority of existing works often focus on routing protocols and do not fully exploit the drones' superiority and flexibility. To fill in this gap, this paper proposes a collaborative communication scheme for multiple drones to assist the urban vehicular ad-hoc networks (VANETs). In this scheme, drones are distributed according to the predicted terrestrial traffic condition in order to efficiently alleviate the inevitable problems of conventional VANETs, such as building obstacle, isolated vehicles, and uneven traffic loading. To effectively coordinate multiple drones simultaneously, this issue is modeled as a multimodal optimization problem to improve the global performance on a certain space. To this end, a succinct swarm-based optimization algorithm, namely Multimodal Nomad Algorithm (MNA) is presented. This algorithm is inspired by the migratory behavior of the nomadic tribes on Mongolia grassland. Based on a real-world floating car data of Chengdu city in China, extensive experiments are carried out to examine the performance of the proposed MNA-optimized drone-assisted VANET considering the processed mobility models. The results demonstrate that our scheme outperforms its counterparts in terms of the average number of hops, improved average packet delivery ratio, and throughput of the global test space.**

***Index Terms*—Drone, Vehicular ad-hoc networks (VANET), Collaborative communication, Multimodal optimization, Multimodal nomad algorithm (MNA).**

I. Introduction

With the rapidly growing numbers of vehicles, the Intelligent Transportation System (ITS) is expected to play a vital role in the future enabling a plethora of applications such as collision avoidance, turning warning, intelligent guidance, and real-time transport information [1] [2] to increase the safety, comfort, and convenience during driving. Most services of ITS rely on connectivity, in which the vehicles can connect to neighbors wirelessly. Data can be generally transmitted between vehicles within the lifetime of the wireless link. However, once the distance between the two vehicles is beyond the communication range, the link will no longer exist. In this context, the dynamic movement of vehicles can cause the frequent change of topology that connectivity of such vast number of vehicles is always intermittent [3]. It is a serious challenge for ITS. Thus, Vehicular ad-hoc networks (VANET) [4] is designed as a special type of mobile ad-hoc networks (MANET) to deal with the above challenge [5, 6]. Besides the frequent changing topology, another challenge of urban VANETs is caused by link quality. Wireless links are applied to connect dynamic vehicles or to the base station, with technologies including 802.11p [7], LTE-V or future 5G-V2X [8] which are sensitive to environmental factors, such as distance, obstacles, as well as a radio signal from other devices. The above issues cannot be easily overcome at the networking level. Therefore, in recent years, researchers have begun to find alternative solutions such as finding assistants like drones to bypass the obstacles and extend the coverage of the infrastructures and vehicles [9].

Recent advances in Unmanned Aerial Vehicles (UAVs), i.e., drones, have attracted many research attentions in networking. The drones hovering in the air are with less constraints, e.g. drones are not constrained to roads. This advantage enables the drones to act with faster and more-directional mobility models. With onboard communication device equipped, it can perform similar network function and link properties to any urban vehicle. Drone plays as a flexible but energy-constrained network node whose action should be meticulous controlled. To achieve real-time communication of drones, the flying ad-hoc networks (FANET) [10] are proposed. In FANETs, drones are expected to provide flexible and fast-deployed network access or relay in complex environments where infrastructure is unavailable such as flood zone, earthquake-stricken area, and accidents [11, 12]. Some key features of this type of air-ground communication are discussed in [13].

Besides these listed scenarios, drones are also shown as a promising player to enhance the connectivity of vehicular networks. For example, the authors in [14] propose a UAV-assisted routing solution for urban VANET. It provides reliable

- *Na Lin, Liang Zhao ({linna, lzhao} @sau.edu.cn), Luwei Fu (luwei.fu2019@gmail.com) are with Shenyang aerospace University; Shenyang, 110136, China; Liang Zhao is the corresponding author.*
- *Geyong Min (g.min@exeter.ac.uk) is with the University of Exeter, UK;*
- *Ahmed Al-Dubai (a.al-dubai@napier.ac.uk) is with School of Computing; Edinburgh Napier University, UK;*
- *Haris Gacanin (harisg@ieee.org) is with Nokia Bell Labs, Antwerp, Belgium;*

routing path and ensures alternative solutions when the path fails. In urban environments, the movement and communication of vehicles are constrained by the buildings and infrastructures [15]. Nevertheless, the height of drones beyond all the terrestrial infrastructures allows the drones arbitrarily to move with much less terrestrial constraints. Moreover, terrestrial obstacles can generate fewer influences on the transmission of drones in the air. All these results in that drones become a suitable assistant for VANET. Based on the above advances, the authors in [16] deploy the drones to detect the incidents on urban road and provides emergency vehicle guidance. A vehicle-drone hybrid ad-hoc network is designed to reduce the end-to-end delay among vehicles [17]. Applying the drones to boost VANETs, some routing protocols with consideration of drone-assistance are proposed in [18-20]. A software-defined network architecture consisting of drones and vehicles are also designed to support various vehicular services in a seamless manner [21].

However, existing studies have shown prominent problems. Some are only proposed as a framework without the appropriate scenario and detailed algorithm [9, 21]. Others focus on routing protocols, omitting the full exploitation of the drones' superiority [18-20]. In fact, all existing drone-assisted schemes rely on the routing protocol to optimize the performance of VANETs. Moreover, although these schemes achieve improvements on some evaluation metrics such as the delivery rate or throughput, there are always tradeoffs between performance metrics for different previous routing proposals. In this work, we aim to design a drone-assisted VANET to boost multifaceted performances of communication without modification of VANET protocols. According to the predicted distribution of the vehicles, our proposal dispatches the drones to the most appropriate locations in real-time. A multi-objective multimodal-based scheme is designed as vital to satisfy complex networking requirements for multi-drone collaboration. However, the existing multimodal optimization technologies are not suitable for our model due to three aspects: high time consumption, uncertain number, and unconstrained distribution of potential solutions [22]. A specialized multimodal optimization algorithm should be developed. The main contributions of this study can be summarized as follows:

1) This paper proposes a novel collaborating network architecture that integrates the drones with VANETs. For a certain position, we define the detailed criterion to evaluate the demand for drones quantitatively. It considers multiple objectives of VANETs and builds an evaluation function for optimization. The purpose of this evaluation function is to find the optimal distribution of multiple drones to assist VANET, which is modeled as a multimodal optimization problem.

2) To improve the above model, this paper designs a specific multimodal optimization algorithm, namely, Multimodal Nomad Algorithm (MNA), inspired by the migratory behavior of the nomadic tribes on the Mongolia prairie. MNA enables the instant dispatching of multiple drones to the best service positions in order to enhance the efficiency of drone-assisted VANETs.

3) A series of the benchmark experiments are conducted to verify the powerful optimization capability of MNA. We also conduct the extensive simulation experiments and test the network performance based on the real map data and the floating car data of Chengdu city, China. The simulation results are discussed and analyzed in detail.

The rest of this paper is structured as follows. Section II describes the collaborative model of the proposed drone-assisted VANET and gives a detailed workflow. In Section III, we transform the collaboration problems into a multimodal optimization and present our Multimodal Nomad Algorithm to solve the problem. The simulations are presented and discussed in Section IV. Finally, the conclusion and future research direction are drawn in the last Section V.

II. System Model

This section firstly gives some assumptions about diverse devices and environment. Then, the architecture and computation models of our system are also illustrated.

A. Assumptions

We ideally assume that all the drones and terrestrial vehicles are equipped with GPS system where their geographic location is aware for themselves and data center. To communicate, all vehicles and drones adopt the 802.11p [7] where the wireless links have bidirectional reachability within the radio range. More, energy consumption is not the primary concern of this study. Drones are distributed in the air beyond all the ground building. Without constraints of buildings, drones can move arbitrarily and line-of-sight (LoS) communicate with any node. Note that we generally suppose the actual communication range between two nodes are determined by the smaller one, if two nodes are with different communication abilities. In addition,

TABLE I
Features Comparison of the Most Related works.

Related work	Application scenario	Basic idea	Major advantage	Limitation
Ref. [14]	Urban VAENT	Predicting the lifetime of path, providing alternative routing.	Reliable routing path	Full coverage of drones required
Ref. [16]	Surveillance, rescue	Deploying drones to detect the incidents.	Suitable for the high mobility and restricted energy scenario	Full coverage of drones required
Ref. [17]	Infrastructure-less VANET	Predicting the destination, using drones deliver data and collect information	Low delay	Each vehicle should be equipped with an on-board drone
Ref. [18]	VANET on two-way highway	Replacing infrastructure with drones	Minimized V2I delay	Only V2I communication on a straight road
Ref. [19]	Urban VANET	Deploying drones to monitor traffic and assist vehicles in routing	Reduced delay and improved delivery ratio	Full coverage of drones required
Ref. [20]	Urban VANET	Applying drones to provide alternative path, and select the optimal path.	Consider the stability and distribution of vehicles during path selecting	Mobility of drones without rational scheduling

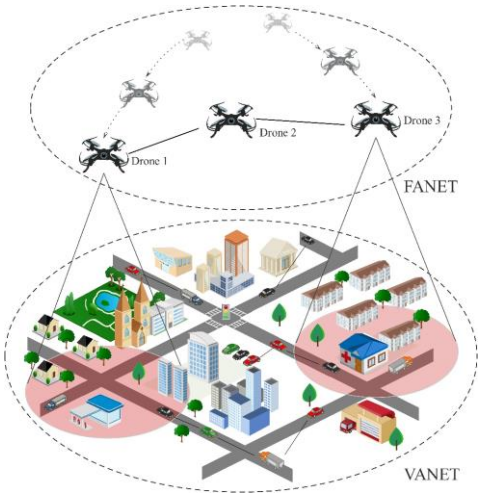

Fig. 1. The architecture of drone-assisted VANETs

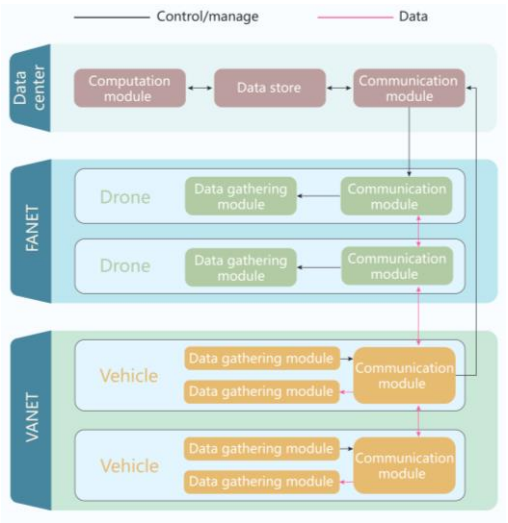

Fig. 2. The structure of drone-assisted VANETs.

drones should have the extra 4G-LTE channel to communicate to the data center (elaborated in Section II.B). This channel is with minor delay and adequately wide range to cover all drones in the task area, which is used to transmit the scheduling instruction from data center to drones. To sum up, 802.11p is applied between drone-to-vehicle (D2V), drone-to-drone (D2D), and vehicle-to-vehicle (V2V) while 4G-LTE is used for the communication of infrastructure-to-drone (I2D) in particular for arranging the schedules of drones from data center.

B. Collaborative Drone-assisted VANET

Existing work has enhanced the VANET by applying drones in many means. However, several limitations should be considered. The key features of the most related works are compared in TABLE I. All these schemes intend to improve the network performance of VANET. Nevertheless, they neglect to consider the mobility superiority of drones which a small number of dynamic drones with rational scheduling can replace many infrastructures work in a wide area. Thus, we consider leveraging dynamic drones to assist VANET according to the distribution of vehicles.

This collaborative networking model consists of two components: the flying ad-hoc networks (FANET) and the vehicular ad-hoc networks (VANET).

FANET is composed of a swarm of drones with wireless communication. These aerial nodes are scheduled by a data center and responsible for providing high-altitude relays. In this architecture, drones never actively request service for communication and only are used as the relay nodes. In other words, it cannot be the source or destination node for routing. However, drones take advantage of flexible mobility to be quickly deployed where relays required. VANET is made up of terrestrial vehicles in urban scenarios.. Compared with drones, the mobility of vehicles is restricted by the road network and traffic regulations. In this context, vehicles can only move along the road rather than free movement, where the velocity, turning, and parking are constrained. Also, due to the wireless links, the surrounding environments impact the qualities of links unavoidably in which the coexistence of a large number of wireless links and obstacles in the city make strong interference to the communication channel of vehicles. Therefore, we should introduce a more effective scheme to alleviate these defects.

We use Fig. 1 to show the architecture of the drone-assisted VANETs in urban environments, where the vehicles can directly connect to neighbors within the communication range wirelessly. To better support the networking in such dynamic networks, *Drone* 1 flies to an appropriate location as a relay node for some vehicles. In that region, two cars are isolated, which means they are far away from other nodes who they relied on to transmit the data messages to the infrastructure or farther. Besides, various buildings and urban infrastructures will be the obstacles and hinder the transmissions. However, compared to the vehicular nodes, drones are much less influenced by the obstacles to make appropriate movement and communication. As a typical case, in Fig. 1, *Drone* 3 relays two vehicles within its coverage, whereas two vehicles are obstructed by a hospital to build connections.

In this architecture, drones are first dispatched to a specific location. When the drones reach the designated positions, they will hover there and act as the relay nodes. To avoid the excessively frequent or infrequent change of drones, the task is divided into a series of time slices. The drones periodically update the destination when a time slice ends. For a certain position, the detailed criterion for assessing the demand of drone is outlined in Section II. C. We first give the structure of our proposed collaborative model by the following Fig. 2.

The data collection module (DCM) and communication module (CM) are designed in each node. The former gathers node's location information periodically with the timestamp, where the latter transmits data to other nodes. The distribution of drones is managed by the data center in which the control instructions are revived by CM and delivered to DCM to correct course. As for vehicles, location acquired in DCM is frequently reported to the data center through CM. To support data center management, the location information with the only micro size is employed to decide the distribution of drones. The data center is responsible for the management of the system. Once the data

center receives the vehicle information through CM, it maintains the information in the data store. The computation module of data center extracts information from the data store to predict the future vehicle distribution and calculates the optimal distribution for drones. The computing results are stored as a series of instructions and periodically transmitted to drones by CM. Afterward, the drones are dispatched to the destination as relay nodes. The packets transmission of D2V, D2D, and V2V are data information. This type of information consists of real required data for on-board applications and services.

For a T drone assisted VANET, we randomly generate T positions over the geographical area at the initialization. Due to the time consumption of the computation and drone deployment, it is improper to evaluate somewhere demand for the drone by current vehicles distribution; the predicted future node distribution should be employed. For data center, all past positions of drones are available with timestamps, which are collected to construct the movement trajectory. We use the historical trajectory to predict the future location of vehicles. It is calculated as:

$$\hat{x}(t_{n+1}) = x(t_n) + \Delta x(t_{n-1}) + \Delta\hat{x}(t_n) \tag{1}$$

where $\hat{x}(t_{n+1})$ is a vector that represents the predicted position of a vehicle, at the beginning of the time slice t_{n+1}. $x(t_n)$ is the real physical position of a vehicle at the beginning of the time slice t_n, while $\Delta x(t_{n-1})$ is the real position change of a vehicle during the time slice t_{n-1}. Note that $\Delta\hat{x}(t_n)$ is a correcting factor to adjust vehicle position during time slice t_n. The available historical trajectory determines this factor. The computational process is shown as following (2) and (3):

$$\Delta x(t_{n-1}) = x(t_n) - x(t_{n-1}) \tag{2}$$

$$\Delta\hat{x}(t_n) = \sum \omega_i \cdot \left(\Delta x(t_{n-i}) - \Delta x(t_{n-i-1})\right) \tag{3}$$

Considering the influence of the past state is decreased, the weight of the previous i-th time slice ω_i should satisfy follows:

$$\sum \omega_i = 1 \tag{4}$$

$$\omega_{i+1} < \omega_i \tag{5}$$

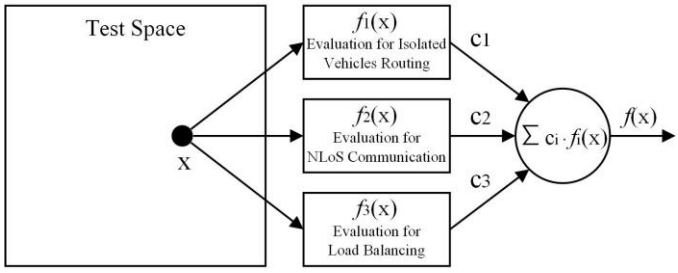

Fig. 3. The combination of multiple objectives.

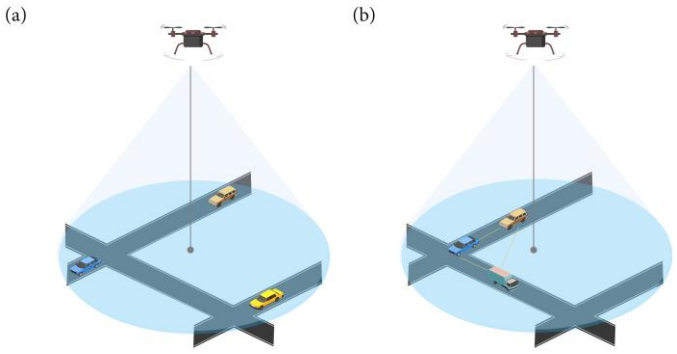

Fig. 4. The difference in dispersion.

It means that the earlier trajectories have less influence weight than the fresher. This prediction has considered the weight discrepancy of the different time slice. By this way, the distribution of the vehicle at the next time slice is predicted with an acceptable error. According to the distribution, we can evaluate the demand (i.e. fitness) for a relay node for a specific geographical area. In this context, the area urgently demands a relay that should be with more considerable fitness. Thus, we search for several optima with the best fitness in the search space, and the number of drones determines the number of optima. Once the system has mapped out the destination for drones in next time slice, each drone quickly flies to the nearest destination and hovers there. Afterward, drones work as relay nodes in the air and wait for a new task in the next time slice.

C. Computation Models

In our drone-assisted VANET, we study how to evaluate the demand for drones subsequently. For optimizing the network performance of urban VANETs, we can apply the drone-assisted scheme in three scenarios, including relaying isolated vehicles routing, assisting No-Line-of-Sight communication (NLoS), and minimizing the network load imbalance. Finding the fittest distribution which provides the best assistance for these three scenarios, is a multi-objective optimization problem. Thus, the above three scenarios are combined to build an evaluation function to assess the demand for drone as (6) and illustrated by Fig. 3.

$$f(x) = c_1 \cdot f_1(x) + c_2 \cdot f_2(x) + c_3 \cdot f_1(x) \tag{6}$$

where x is a vector represents a position to be evaluated in test space, $f(\cdot)$ is the evaluation function. To satisfy multiple requirements simultaneously, $f(\cdot)$ consists of 3 subordinate functions f_1, f_2 and f_3 used to assess the three aspects mentioned earlier. All these functions are normalized to the

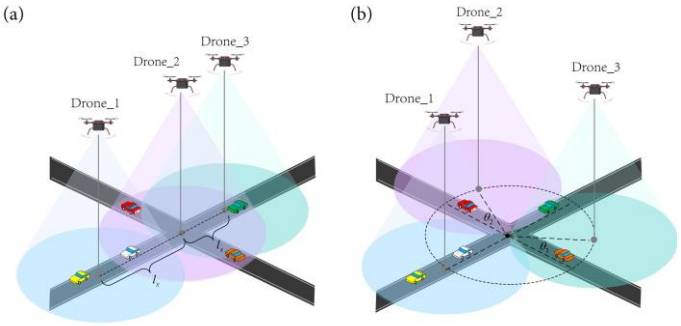

Fig. 5. The comparison of drones in different locations.

range (0, 1). c_1, c_2, and c_3 are their impact weights respectively, where the sum of them is 1.

Considering a more abundant connection is the primary prerequisite of VANET, the weights of f_1 and f_2 should be taken major accounts in this problem. Because the '*load balancing'* relies on the network connectivity, and if there are a lot of disconnected nodes, it is meaningless to maintain load balance. Furthermore, although communication between vehicles close to intersection is hindered by obstacles, it is still possible for transmission with impaired probability. However, for an isolated vehicle, it is absolutely impossible to connect with any other nodes by itself. Therefore, the urgency of f_1 should be taken greater account than f_2. The final impact weights of these 3 objectives (c_1, c_2, and c_3) are 0.5, 0.35, and 0.15, respectively. We will discuss each scenario in detail in the following subsections.

1) The Isolated Vehicles Routing

For the outlier vehicles or isolated area, relay nodes are urgently needed. In other words, if some vehicles are far away from each other but within the radio range of a drone, that is a suitable position for drone deployment. This condition is shown in Fig. 4.

In Fig. 4(a), if the vehicles have the same communication range as drones, the distances between each two vehicle nodes are beyond the radio range; they are unable to connect. The vehicle nodes in Fig. 4(a) can be seen as isolated nodes without neighbors. However, all of them are in the communication range of a drone; the message can be transmitted by the drone relay node. In contrast, the vehicles in Fig. 4(b) are close to each other; links can be normally established. It is unnecessary to introduce drone assistance in condition (b). Additionally, the vehicles further away from the drone are with greater risks of disconnection in later period. For instance in condition (a), subsequently, these vehicles are likely to go beyond the communication range of drone and become isolated nodes again. Thus we define the evaluation criterion as

$$f_1(x) = \frac{1}{n} \cdot \sum_{i=1}^{n} \frac{\|X_i - \bar{X}\|_2}{R_d} \cdot e^{-\frac{\|X_i - x\|_2}{R_d}} \tag{7}$$

where n is the number of vehicles within the radio range of the drone. $\bar{X}$ is the average position of n vehicles. X_i denotes the geographical position of the i-th vehicle. x represents a position to be evaluated, i.e., a potential destination for the drone. $\|\cdot\|_2$ is an operator to calculate the 2-norm which also be regarded as the Euclidean distance between two positions. The R_d is the radio radius of drone, which is introduced to normalize the computational result into the range (0, 1). Equation (7) has considered both the discreteness among vehicles, and the discreteness of vehicles to drone. Within the radio range of a given position *x*, it represents the better fitness of position *x* for drone deployment if the vehicles are further away from each other and the vehicles are closer to *x*.

2) Non-line-of-sight Communication

In the urban VANETs, the buildings and various infrastructures are ubiquitous where these obstacles inevitably obstruct the message transmission in wireless links. This non-line-of-sight (NLoS) communication with severe loss always leads to failed transmission. While a vehicle node sends messages to another vehicle located on the adjacent road segment, the transmission has to bypass the building between the two segments which is infeasible with high packet dropping. Therefore, although this distance between the two nodes is not beyond the range of wireless, the message is challenging to deliver. Regarding NLoS communication, the drone-assisted network is suitable to forward the message as a relay node. The drones hover in the high altitude beyond the most obstacles and even perform the store-carry-forward in which the obstacles can hardly disturb the movement and communication of drones. The links of D2D and D2V are referred as the Line-of-Sight (LoS) communication without obstacles. Thus, we consider the condition that vehicles near the intersection communicate with vehicle in adjacent road segments.

Fig. 5 gives the comparison while the drones at a different location. As shown in Fig. 5(a), the closer the drone is to the intersection, the larger area of the road it can cover. In the extreme case, *Drone*_1 is so far to the intersection that it can only cover the road segment which itself located. It only assists vehicles within the same road, whereas it is meaningless because these vehicles can communicate by themselves. In another extreme case, the *Drone*_2 in Fig. 5(a) is closest to the intersection and exactly located there. This drone evenly covers all adjacent segments around the intersection and can provide the relay links for vehicles in every two segments. Fig. 5(b) reveals the effects by different angle when the distances to the intersection are fixed. We define the the θ between the lines from drones to intersection and drone's nearest segment. According to the auxiliary circle whose center located at intersection and radius is equal to radio range of the drone, these three drones have the same distance to the intersection. However, *Drone*_1 has no angle to the segment in which it can only cover one segment, i.e., it is useless for helping the vehicle communicate with nodes which are located at other segments. By contrast, *Drone*_2 has a larger angle to the nearest segment where it covers two segments but unsymmetrically. This drone can play as an aerial relay node to alleviating the building obstacles in slight measure. Therefore, we consider that if the angle between the nearest segment and drone to the intersection is as large as possible (e.g., *Drone*_3 has largest π/4 angle), such position is the best location for drone deployment.

Based on the above discussion, the preliminary evaluation function $g(x)$ is defined as follows

$$g(x)=\begin{cases}0 & l_x > R_d \\ \dfrac{R_d - l_x}{R_d} + \omega \cdot \dfrac{l_x}{R_d} \cdot \cos\left(\theta - \dfrac{\pi}{4}\right) & l_x \le R_d\end{cases} \tag{8}$$

where l_x is the distance between the objective position x and nearest intersection. If l_x is beyond R_d, the drones can cover one segment at most, it is meaningless for overcoming the communication obstacles. ω is a controlling factor used to adjust the weight proportion of the distance to angle. Equation (8) represents that the fitness (value of evaluation function) will increase when the objective position is closer to the intersection with a larger angle θ. The influence of angle will shrink with the decrease of the distance l_x. For instance, whatever the value of θ is, there is no difference when the objective position is located at intersection (i.e., $l_x = 0$). To unify the evaluation standard, the value of $g(x)$ should be normalized into the range (0, 1) to construct the final evaluation function $f_2(x)$ by (9):

$$f_2(x)=\begin{cases}0 & g(x)=0 \\ \dfrac{g(x) - \omega \cdot \cos\frac{\pi}{4}}{1 - \omega \cdot \cos\frac{\pi}{4}} & g(x)\neq 0\end{cases} \tag{9}$$

3) Load Balancing

Due to the huge number of vehicles and complicated traffic conditions in urban traffic, the network quality is unstable. However, many onboard services significantly rely on the network quality, such as infotainment applications, and safety driving applications. When the distribution of the vehicles becomes dense, the overhead of the network will dramatically increase in this area. Consequently, the load gets heavy that especially of the edge nodes.

To further satisfy more requirements for service, great network quality is also necessary for this architecture. Considering the extremely high-density vehicles will take a heavy load to the edge nodes, meanwhile too sparse may lead to the lack of relay in the forthcoming mission, we define the evaluation function as follows:

$$f_3(x)=\frac{\left|N_x - N_{\text{avg}}\right|}{\max\left(N_{\text{avg}}, \left(\max(N_i) - N_{\text{avg}}\right)\right)} \tag{10}$$

where N_x and N_i represent the number of vehicles within the radio range (R_d) of the objective position x and i-th drone, respectively. max(·) is a function to get the maximum. N_{avg} is the average number of vehicles around a drone, and it is calculated by Equation (11) as

$$N_{\text{avg}}=\frac{\pi {R_d}^2 \cdot N_{\text{total}}}{S_{\text{total}}} \tag{11}$$

where N_{total} and S_{total} indicate the total size of vehicles number and simulation area, respectively. This mechanism guarantees the value of $f_3(x)$ within the range (0, 1) and get increasing at locations with too many or too few vehicles. By this way, the drones are more likely to be dispatched to the extreme congested or desolate road segment.

Thus, the multi-objective evaluation function (6) has been built on the basis of (7)-(11). The value range of evaluation function is (0, 1) while greater value means higher demands for drone-assisting.

III. Multimodal Optimization for Communication

In the previous section, the evaluation standard has been established for selecting appropriate positions for multiple drones. The original problem is transferred to a multimodal optimization problem, aiming to locate multiple optima in a search space. However, conventional multimodal optimization technologies cannot provide feasible solutions for our problem, while the reasons will be discussed in the forthcoming subsection. Afterward, we design a specialized multimodal optimization algorithm, Multimodal Nomad Algorithm (MNA). Comparison experiments are also conducted to verify the effectiveness of our proposal. Finally, the workflow of MNA-optimized drone-assisted VANET is also presented in detail.

A. Motivation and Inspiration Source of MNA

To solve our formulated problem, there are three constraints should be satisfied simultaneously. Firstly, our drone-assisted VANET should operate in real-time with strict requirements for computation time. Moreover, each optimum of multimodal optimization indicates a deployment location of a drone, that is, we need a specified number (depending on the number of available drones) of different optima. Lastly, considering the multiple adjacent drones only redundantly play the same role, their locations (different optima) should keep a distance from others. Having reviewed and concluded various multimodal algorithms in TABLE II, it has been found that they are inapplicable to this problem [23-28]. Part of these algorithms [24-27] are time-consuming due to the repetitious sorting and distance measuring. Otherwise, the majority of multimodal

TABLE II
FEATURES COMPARISON OF THE EXISTING MULTIMODAL ALGORITHM.

	Ref. [23]	Ref. [24]	Ref. [25]	Ref. [26]	Ref. [27]	Ref. [28]	Required
Low time consumption	√	×	×	×	×	√	√
Specified number of optima	×	×	√	×	×	√	√
Constrained distance between different optima	×	√	√	√	√	×	√

Algorithm 1 Herdsmen Grazing

Input: The current iteration t, the position of i-th tribe X_i, the fitness of i-th tribe $f_i(t)$;
Output: The position of Herdsmen;
Calculate the number of Herdsmen M_H by **(12)**;
Calculate the grazing radius $R_i(t)$ by **(14)**;
for each Herdsman **do**
  for each dimension **do**
    X^k=$X_i{}^k$ + Rand$(-R_i(t), R_i(t))$;
    // Avoid searching beyond boundaries
    if $X^k < X_{min}{}^k$ **or** $X^k > X_{max}{}^k$ **then**
      X^k=Rand$(X_{min}{}^k, X_{max}{}^k)$;
    end if
  end
end

algorithms are Niching-based [22], which require prior knowledge to specify niching parameters or cannot constrain the number and distance of optima simultaneously. Thus, the form of solutions found by existing algorithms does not match the requirements of our scenario.

To design the feasible algorithm for the scenario of collaborative communication, we propose an efficient multimodal optimization algorithm called Multimodal Nomad Algorithm (MNA), which is inspired by the migratory behavior of nomadic tribes on the Mongolia grassland. Nomadic tribes are known for their migratory behavior, who always seek and regularly migrate to a more suitable place with lush pasture. Once they settle somewhere, herdsmen live and work around the tribe within a specific range which depends on the fitness of the environment. To avoid stagnation at somewhere and exhaustion of resources, some members are selected as Rangers to explore. Rangers can quickly explore a farther area for a better environment. For peaceful coexistence, various tribes will not intrude into other tribes' territories when they migrate. These processes can be mathematically modeled to design our intelligent optimization algorithm.

In MNA, the migrating process of nomadic tribes can be regarded as the search process of the algorithm. The most habitable places are considered the multiple best solutions, and the vast grassland is treated as a search space. All members of each tribe can be divided into two types: Herdsmen and Rangers. Herdsmen and Rangers are responsible for local exploitation and global exploration, respectively. Hence, the MNA consists of Herdsmen grazing, Rangers exploring, and migration determining strategies. This algorithm has a very succinct and powerful search mechanism, which predefined the required number and minimum spacing of optima. It quickly obtains a known number of most appropriate positions for drones. This distribution of drones enhances VANET in varies metrics.

B. Design of MNA

The proportion of the two types of members in each tribe will determine the balance between both global exploration and local exploitation. The numbers of Herdsmen, denoted by M_H is defined (taking the integer portion) as

$$M_H = M \times \left(max_P - \frac{(max_P - min_P) \times t}{Max\_ite} \right) \tag{12}$$

where M indicates the population size of MNA, max_P and min_P are the maximum and minimum proportion of Herdsmen in population, respectively. Max_ite is the maximum iterations of MNA. These parameters are predefined at initialization. Note that t represents the current iteration times, which grows with the running of the algorithm. Besides Herdsmen, other members are employed as Rangers, whose number M_R is calculated as follows.

$$M_R = M - M_H \tag{13}$$

To start the computation, the grazing radius is set to be big enough to widely search a potential space, in place of Rangers global exploring. With the execution of the algorithm, the grazing radius will be reduced gradually to a narrow range, which enhances the exploitation capability, while the global search capability has declined. Thus, more Rangers need to be picked to balance exploration.

We stipulate that a tribe always located in the most liveable territory it found (somewhere with higher fitness). The territory of the i-th tribe in the search space is defined as a d-dimensional vector $X_i = \{x^1, x^2 \cdots x^d\}$, where each dimension represents a parameter of an objective function to be optimized. In other words, a tribe denotes a current optimal solution in the search space. It is generated randomly in the initialization of MNA and updated in each iteration. The herdsmen work near the tribe within a certain radius in each iteration. The grazing radius is calculated as

$$R_i(t) = \begin{cases} X_{max} - X_{min} & t = 1 \\ R_i(t-1) \times \alpha & f_i(t) > f_i(t-1) \\ R_i(t-1) \times \beta & f_i(t) = f_i(t-1) \end{cases} \tag{14}$$

where $R_i(t)$ is the grazing radius of i-th tribe at iteration t. X_{max} and X_{min} denote the upper and lower bounds of the search space. α is the growth factor, which is higher than 1, and β is the reduction factor greater than 0 and less than 1. Too big or too small values will break the robustness of the search process. Through experimental comparison, we find when α is 1.1 and β is 0.9 could show satisfactory performance for most problems. $f_i(t)$ represents the fitness of the position of the i-th tribe, i.e., the value of the best solution at iteration t.

Equation (14) denotes that the exploit range should be set as the whole search space at the initialization. For i-th tribe, if a better solution is found, this new spot is more suitable to live, and Herdsmen could work on broader space; the search radius should be enlarged in next iteration to search more space. Conversely, if no better solution is found in this iteration, Herdsmen have to reduce their live range to make the search more detailed in the next iteration. These strategies provide more probability to find a better solution and accelerate convergence.

Algorithm 2 Ranger Exploring

Input: The current iteration t, the position of i-th tribe X_i, the fitness of i-th tribe $f_i(t)$;
Output: The position of Rangers;
Calculate the number of Herdsmen M_R by **(13)**;
Calculate the exploring amplitude $\sigma_i(t)$ by **(16)**;
for each Ranger **do**
  for each dimension **do**
    X^k=$X_i{}^k + \mathrm{N}(0, \sigma_i(t)^2)$;
    // Avoid searching beyond boundaries
    if $X^k < X_{min}{}^k$ **or** $X^k > X_{max}{}^k$ **then**
      X^k=Rand$(X_{min}{}^k, X_{max}{}^k)$;
    end if
  end
end

The pseudocode of the Herdsmen as mentioned above grazing is given by **Algorithm 1**. $X_{min}{}^k$ and $X_{max}{}^k$ are the lower and upper bounds on k-th dimension of search space. $\mathrm{Rand}(A, B)$ is a function used to uniformly generate a random number between A and B. Herdsmen randomly search the vicinity of X_i within the radius $R_i(t)$.

Herdsmen grazing process could guarantee the local exploitability of the MNA at the vicinity of the present best solution. However, it is not enough to make the tribe find the most livable place. Somewhere seems to be better than other adjoining areas but is not the best position in the entire search space, which is called local optimum. In order to avoid stagnating at local optimum, we send Rangers to explore more extensive areas. The Rangers have global search capability and search in the entire space according to the present location of the tribe. This behavior of Rangers can be briefly represented as follows:

$$X_{Ranger} \sim N(X_i\ ,\ \sigma_i{}^2) \tag{15}$$

The position of Rangers' exploring X_{Ranger} complies with a Gaussian distribution $N(X_i\ ,\ \sigma_i{}^2)$ with X_i as the mean value and $\sigma_i{}^2$ as the standard deviation. $\sigma_i(t)$ determines the exploring amplitude of i-th tribe's Rangers at iteration t. It is calculated by (16)

$$\sigma_i(t) = \begin{cases} X_{max} - X_{min} & t = 1 \\ \sigma_i(t-1) \times 0.5 & f_i(t) = f_i(t-1) \\ X_{max} - X_{min} & f_i(t) > f_i(t-1) \end{cases} \tag{16}$$

Algorithm 3 Migration Determining

Input: The i-th tribe's new best position X_b and its fitness;
Output: The position of i-th X_i and its fitness $f_i(t)$;
Calculate the $d_{i,b}$ by **(17)**;
for every other tribe X_j **do**
  Calculate the $d_{b,j}$ by **(17)**;
  if $d_{i,b} > d_{b,j}$ **or** $d_{b,j} < \gamma \cdot (X_{max} - X_{min})$ **then**
    End the **Algorithm 3** without any operation;
  end
end
Update X_i and $f_i(t)$

This process can be abstracted as a Gaussian probability sampling. To begin with, exploring amplitude σ is set as the size of the search space. During the computation process, it will rapidly reduce if no better solution found at the previous iteration. Once the Rangers find somewhere with better fitness, the exploring amplitude σ return to the original range. Diverse from Herdsmen which employ the uniform distribution within a certain range, this type of Gaussian distribution has higher search probability on the closer region, also has a probability to search any position within the search space.

The pseudocode of the above process is given as following **Algorithm 2**. $\mathrm{N}(A, B)$ is a function used to generate a random number accord with the Gauss distribution whose mean value is A and variance is B.

Compared with other traditional perturbation or mutation strategies, this method has several advantages. Firstly, many strategies use fixed random perturbation without heuristic information, which does not facilitate intelligence. Secondly, some perturb strategies multiply the current coordinates by a perturbation factor as a new position. The perturbation factor usually follows a certain probability distribution, such as Gaussian distribution or Levy distribution. These strategies often cause a tendency shrinking to origin. The reason for their acceptable test results is that optima of most benchmark functions exactly locate at the zero points. These traditional strategies, however, are infeasible when dealing with those functions built to solve practical problems, whose optima are hardly at the origin.

The Nomad tribe tends to migrate to the best position which has been found. However, there are many tribes coexist on the grassland; a tribe should avoid intruding into the territories of other tribes during its migration. If Ranger or Herdsmen have found a better objective (i.e. location) and this location is close to other tribes, they do not migrate. In other words, the tribe should determine whether the objective position belongs to another tribe before migration. The Euclidean distance is used as the criterion likes (17):

$$d_{i,j} = \left\| X_i - X_j \right\|_2 \tag{17}$$

where $d_{i,j}$ is the Euclidean distance between two position X_i and X_j. When the i-th nomad tribe finishes the search of the current iteration and gets another best position X_b, the migration determining is adopted by **Algorithm 3**.

According to this algorithm, if the objective position found by a tribe is closer to another tribe than to itself, or too close to other tribes, it does not update the position although there are more suitable for living. The γ is a coefficient to determine the boundary of a tribe's territory, i.e., the minimum distance between two different tribes. This mechanism could avoid the multiple tribes falling into similar solutions. Based on the above expressions and algorithms, the architecture of MNA is established. It is constituted of Herdsmen grazing, Rangers exploring and Migration determining processes. We assume that the population size of a tribe is set to N, and the number of

Nomad tribes T is determined by the problem to be solved. If the algorithm ends in t generation, the time complexity is simplified to $O(t \times T \times N)$. The complete process is given by **Algorithm 4**.

Algorithm 4 Multimodal Nomad Algorithm

Input: The search space, dimensions, the objective function of the problem, required number of solution, and the parameters of MNA;
Output: The multiple solutions and their value;
Initialize parameters of MNA;
do
  for each tribe **do**
    Herdsmen grazing by **Algorithm 1**;
    Rangers exploring by **Algorithm 2**;
    Evaluate each member' s fitness;
    Select the best one as X_b;
    Migration determining by **Algorithm 3**;
  end
  Iterations**++**;
until getting the expected precision or maximum iterations;
return coordinates and fitness of all tribes as multiple optima;

C. Efficiency Verification

In this part, comparison experiments are conducted to analyze our proposal. Comparing MNA with other niching-based multimodal algorithms are infeasible due to all these algorithms are constructed in different forms. Hence, only the optimization accuracy and speed on global space are considered for simulation. We select five well-known algorithms as competitors, which are widely applied in the field of industrial optimization, Particle Swarm Optimization (PSO) [29], Gravitational Search Algorithm (GSA) [30], Flower Pollination Algorithm (FPA) [31], Whale Optimization Algorithm (WOA) [32], and Crow Search Algorithm (CSA) [33].

Owing to the common searching strategy of each tribe in MNA, a single tribe's behavior is an independent algorithm to demonstrate the optimization capability. With the same population size, we set a single tribe against other algorithms. As given in Table III, twelve well-known benchmark functions are utilized to verify the effectiveness of algorithms.

The Dim represents the dimensions of each function, i.e., the number of parameters determines the result of the problem. The range indicates the size of the search space. The unimodal functions ($f_1 - f_4$) with high dimensions can examine the exploitation ability of algorithms. In contrast, the multimodal functions ($f_5 - f_{12}$) with quite many local optima can examine the exploration ability and local optima avoidance of algorithms.

Due to the indeterminacy of swarm-based intelligence algorithms, multiple independent experiments should be conducted to reduce the accidental error. With 30,000 times of evaluation, **Table IV** gives the statistical mean (Mean) and standard deviation (Std) of error value optimized by different algorithms over 50 independent runs. The best results for each benchmark function are marked in bold in the table. It shows that MNA has the best accuracy on all the twelve benchmark functions. Apart from f_{10}, MNA also achieves the minimum standard deviations on most functions. With the same evaluation times, it is clear that MNA outperforms other algorithms in optimization accuracy and stability. This superiority means that MNA can obtain better solutions for most problems under the same computation burden. To further study the convergence, more evaluations (300,000) are utilized.

Algorithm 5 MNA-optimized Drone-assisted VANETs

Input: The range of simulation area (X_{min}, X_{max}), the objective function **(6)**, the required number of drones T;
Output: The positions in time for T drones;
Randomly initialize T positions as drones;
do
  Predict the distribution of vehicles in next time slice by **(1-3)**;
  Built the evaluation function **(6)** by **(7-11)**;
  Perform the MNA by **Algorithm 4** to get T global optima;
  Assign optimal positions for T drones by SA that makes the total path shortest;
  T drones respectively fly to their destinations;
  Drones hover at the designated position until the current time slice is exhausted;
until Terminate condition is satisfied
end

The convergence curves of these six algorithms on each benchmark test function also have been shown in Fig. 6. MNA gets the best accuracy on all the 12 benchmark functions. For unimodal functions $f_1 - f_4$, the accuracy of MNA is far more than others, especially for f_1, f_2 and f_4, curves keep a downward tendency, and they will descend to better accuracy with more evaluations. It demonstrates MNA's powerful exploitation capability in local search. In the cases of multimodal functions $f_5 - f_{12}$, MNA also rapidly finds the global optimum with extreme accuracy. Some convergence curves sharply descend and perpendicularly intersect with the horizontal axis (e.g., MNA on $f_{10} - f_{12}$). It means that the algorithm gets the highest accuracy solution under the computer's machine epsilon at current evaluations. Although FPA and CSA get the same best accuracy as MNA on $f_{10} - f_{12}$ whose dimensions are fixed and low, their disadvantage in most conditions represents they are feeble in practices. In all the rest of cases, MNA is superior to its competitors on both convergence speed and accuracy. These experiments and discussions have verified that MNA is an efficient optimization algorithm who can quickly obtain extreme high accuracy in a complex problem.

D. Optimize the Drone-assisted VANETs by MNA

The drone-assisted VANET deploys multiple drones on different positions which have high demands for assistant nodes. It is a typical multimodal optimization problem, and our proposed MNA can be applied for this architecture. The parameters setting of MNA should refer to the requirements of this application. Thus, we set the number of tribes T equals to the number of drones, the bounds of the search space, X_{max} and X_{min}, are determined by the simulation area.

Obviously, our scheme is designed for infrastructure-less scenarios, which results in a shortage of the relay nodes. If the number of drones is sufficient for full coverage, the position of drones could be fixed without the necessity of scheduling. T should be less than that the required number for full coverage, which is calculated as follows:

TABLE III
THE BENCHMARK TEST FUNCTIONS.

Function	Formulation	Dim	Range
Sphere	$f_1 = \sum_{i=1}^{D} {x_i}^2$	30	[-100,100]
Axis Parallel Hyper Ellipsoid	$f_2 = \sum_{i=1}^{D} i{x_i}^2$	30	[-100,100]
Rotated Hyper Ellipsoid	$f_3 = \sum_{i=1}^{D} \left(\sum_{j=1}^{i} {x_j}^2\right)^2$	30	[-100,100]
Schwefel 2.22	$f_4 = \sum_{i=1}^{D} \lvert x_i \rvert + \prod_{i=1}^{D} \lvert x_i \rvert$	30	[-100,100]
Griewank	$f_5 = 1 + \sum_{i=1}^{D} \frac{{x_i}^2}{4000} - \prod_{i=1}^{D} \cos\left(\frac{x_i}{\sqrt{i}}\right)$	30	[-600,600]
Rosenbrock	$f_6 = \sum_{i=1}^{D-1} 100({x_i}^2 - x_{i+1})^2 + (1 - x_i)^2$	30	[-15,15]
Ackley	$f_7 = 20 + e - 20\exp\left(-0.2\sqrt{\frac{1}{D}\sum_{i=1}^{D} {x_i}^2}\right) - exp\left(\frac{1}{D}\sum_{i=1}^{D} \cos(2\pi x_i)\right)$	30	[-32,32]
Schwefel 2.26	$f_8 = D * 418.9829 + \sum_{i=1}^{D} -x_i \sin(\sqrt{\lvert x_i \rvert})$	30	[-500,500]
Rastrigin	$f_9 = \sum_{i=1}^{D} ({x_i}^2 - 10\cos(2\pi x_i) + 10)$	30	[-15,15]
Schaffer	$f_{10} = \left(\sin^2\left(\sqrt{{x_1}^2 + {x_2}^2}\right) - 0.5\right) / \left(1 + 0.001({x_1}^2 + {x_2}^2)\right)^2 + 0.5$	2	[-100,100]
Drop Wave	$f_{11} = -\left(1 + \cos\left(12\sqrt{{x_1}^2 + {x_2}^2}\right)\right) / (0.5({x_1}^2 + {x_2}^2) + 2)$	2	[-5.12,5.12]
Easom	$f_{12} = -\cos(x_1) * \cos(x_2) * \exp(-(x_1 - \pi)^2 - (x_2 - \pi)^2)$	2	[-100,100]

TABLE IV
MEAN AND STD OF ERROR VALUE OPTIMIZED BY MNA, PSO, GSA, FPA, WOA, AND CSA.

Function	MNA Mean (Std)	PSO Mean (Std)	GSA Mean (Std)	FPA Mean (Std)	WOA Mean (Std)	CSA Mean (Std)
f_1	**0.000000 (0.000000)**	2.004647 (0.728381)	**0.000000 (0.000000)**	1834.600 (714.4833)	8.233581 (3.746787)	259.7336 (148.2135)
f_2	**0.000000 (0.000000)**	24.14500 (9.458851)	**0.000000 (0.000000)**	13841.341 (3710.609)	167.7244 (114.4379)	3366.529 (1009.984)
f_3	**0.000000 (0.000000)**	323.8981 (794.4772)	1254.705 (587.0469)	1313.523 (689.3279)	28939.25 (9919.102)	5.7982e+8 (2.8135e+8)
f_4	**0.002367 (0.000731)**	6.638470 (4.983921)	136.4034 (41.05784)	1.850e+11 (1.849e+11)	1.310373 (0.398997)	4.4097e+9 (2.3405e+9)
f_5	**0.008867 (0.006979)**	0.111006 (0.047333)	45.74147 (10.25388)	12.18651 (3.648560)	1.069219 (0.024095)	2.469631 (0.988741)
f_6	**17.03999 (7.054571)**	2161.197 (5692.326)	28.60900 (8.393017)	2871.898 (1830.691)	27.19862 (0.535644)	1209.539 (188.2314)
f_7	**0.000189 (0.000101)**	2.485380 (0.348010)	0.165836 (0.077859)	15.09203 (2.025805)	5.756136 (1.255586)	4.968268 (1.233254)
f_8	**0.000385 (0.000006)**	5935.619 (889.1302)	9954.876 (585.3515)	5238.598 (200.2004)	1177.963 (1622.258)	8123.234 (7881.231)
f_9	**0.602605 (0.491013)**	154.2373 (30.03182)	29.84874 (7.612125)	246.9591 (23.54817)	107.9073 (35.27835)	245.0780 (128.2357)
f_{10}	**0.006477 (0.004580)**	0.009434 (0.003884)	0.026764 (0.036737)	0.00839 (0.001713)	0.007125 (0.004296)	0.007286 (0.00628)
f_{11}	**0.000000 (0.000000)**	**0.000000 (0.000000)**	0.009682 (0.015221)	**0.000000 (0.000000)**	0.017001 (0.028193)	**0.000000 (0.000000)**
f_{12}	**0.000000 (0.000000)**	**0.000000 (0.000000)**	0.793226 (0.349634)	0.000118 (0.000272)	0.133333 (0.339934)	**0.000000 (0.000000)**

$$T_{fc} = \left(\left\lceil \frac{Len}{R_d} \right\rceil - 1\right) \cdot \left(\left\lceil \frac{Wid}{R_d} \right\rceil - 1\right) \tag{18}$$

where Len and Wid are length and width of the rectangle task area, respectively. R_d represents the communication range of drones. T_{fc} indicates the minimum number of drones for fully covering the task area, where drones are uniformly dispersed.

Moreover, the total consumption of time and energy for drones should be considered for minimization. When the algorithm obtains new positions as many as the number of drones, a sequence should be built to indicate each drone flies to which destination. As assigned by this sequence, the total distance of all drones from the original position to their destination will be minimized. This requirement can be reduced to a Traveling Salesman Problem (TSP) and solved by standard Simulated Annealing (SA) [34].

The pseudocode of MNA-optimized drone-assisted VANET is abstracted as following **Algorithm 5.** By this mechanism, this drone-assisted communication system can run continuously in

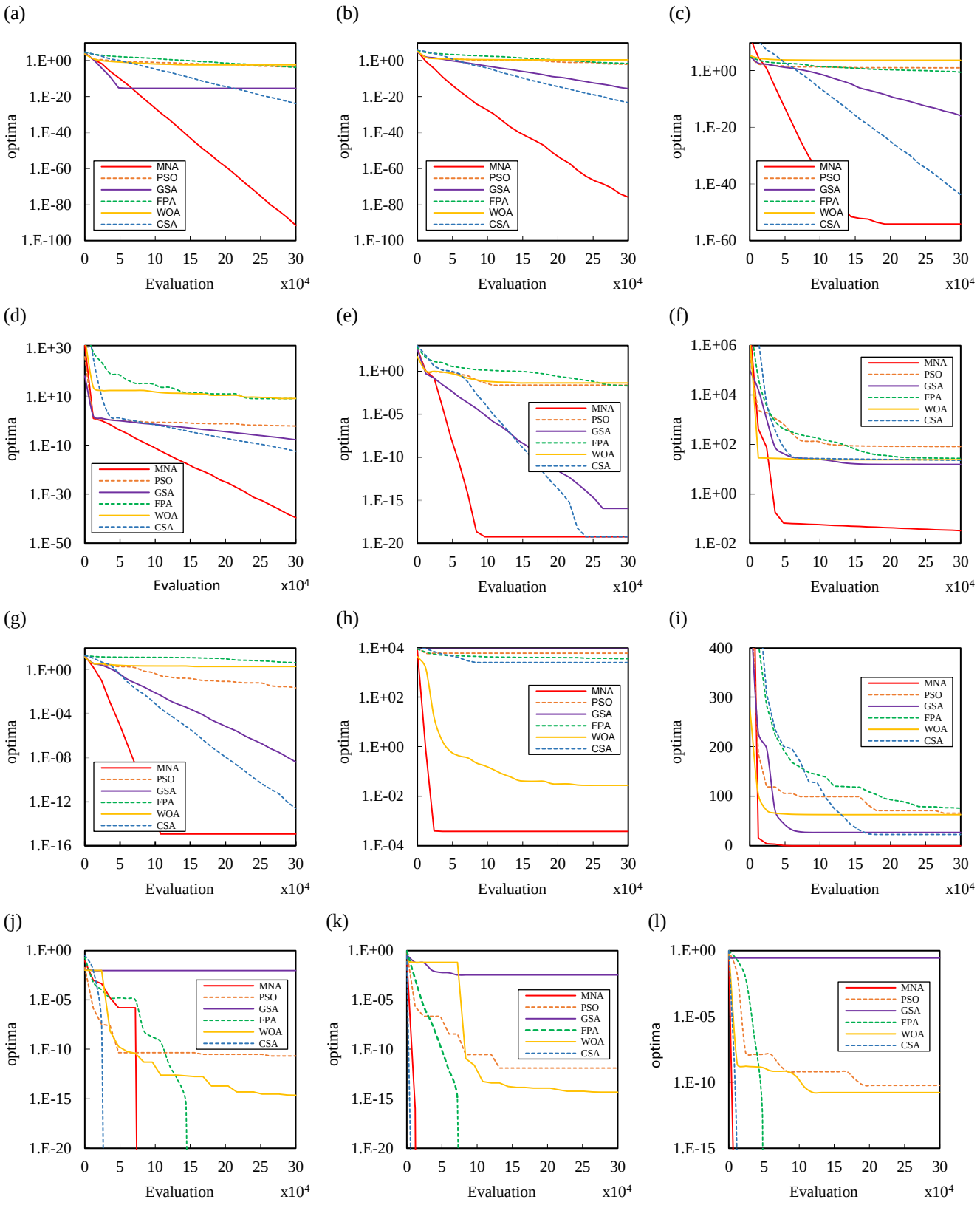

Fig. 6. Convergence curves of MNA, PSO, ABC, FPA, WOA, and CSA on benchmark functions. (a) Sphere function; (b) Axis Parallel Hyper Ellipsoid function; (c) Rotated Hyper Ellipsoid function; (d) Schwefel-2.22 function; (e) Griewank function; (f) Rosenbrock function;(g) Ackley function; (h) Schwefel-M function; (i) Ackley function; (j) Schwefel-2.26 function; (k) Drop Wave function; (l) Easom function;

real-time. During the whole conduction of this system, drones always have communication capability as relay nodes, whether they are moving or hovering. In any time slice, the drone-assisted VANET model predicts the distribution of future

vehicles according to the movement of current a such as current positions and velocities. Based on the predicted distribution of vehicles, the fitness of arbitrary position, which means the demands for drone assistance, can be evaluated by our model. Afterward, the MNA is conducted to obtain multiple global optimal solutions, i.e., the expected locations for drones. This rational dispatching of drone relays brings significant improvement to terrestrial VANET communication.

IV. Simulation and Model Validation

In this section, we show the simulations conducted to evaluate the efficiency of our model. The proposed MNA-optimized drone-assisted (MNAD) VANET is compared to three VANET schemes. First, as the baseline, the conventional VANET with No Drone-assisted (ND) are compared. Second, the Fixed Drones-assisted (FD) VANET is utilized likes infrastructures, which show why VANETs need drones rather than base stations. Last, the Cruising Drones-assisted (CD) VANET is set as one counterpart to evaluate MNA. The CD evenly divided task area into T (the number of drones) sub-areas, while each drone flies within one sub-area with a smooth random walk mobility model [35]. By applying the same routing protocol, our proposal enhances VANETs on multifarious network performance. Considering our proposal aims to enhance network performance but is independent from routing protocols, four evaluation metrics of the network are adopted to simulation including packet delivery ratio (*PDR*), end-to-end delay (*EED*), the average number of hops (*HOPs*), and throughput.

A. Simulation Environment and Parameters

All the network simulations are implemented by NS-2 [36] where the well-known AODV [37] is applied as the routing protocol. To make our simulations approaching the real urban scenario, we adopt the real geographic data provided by OpenStreetMap [38] and relevant floating car data provided by Didi [39]. Due to the low density of floating car data, unprocessed data are unsuitable for network simulation. According to 1,000,000 floating car data corresponding to the simulation area, we make a statistic to obtain the motion features, including the maximum parking time, the maximum, minimum, and average speeds. These features and map data are delivered to SUMO [40] to generate the vehicle mobility model. The downtown of a prosperous city (Chengdu City, China) is modeled as following Fig. 7, in which the simulation parameters are summarized in Table V. To avoid the accidental discrepancy and get meaningful statistical results, 30 independent runs are conducted for each simulation scenario to calculate the average value.

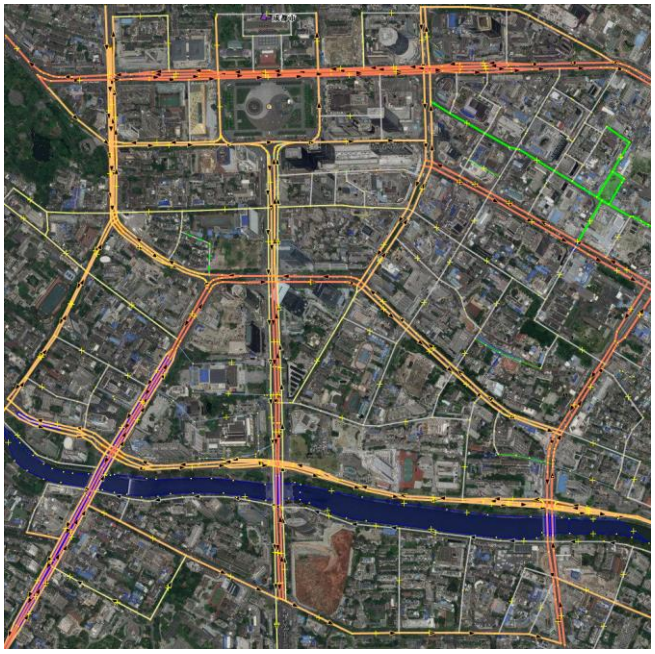

Fig. 7. The simulation area.

TABLE V
Simulation Parameters

Parameters	Value
Simulation scenario	
Simulation area	2000 m × 2000 m
Simulation time	180 s
Mobility generator	SUMO [34]
Number of road segments	208
Number of intersections	102
Number of vehicles	100, 200
Number of drones	4, 8, 12, 16, 20
Vehicles speed	0-60 km/h
Drone speed	0-90 km/h
Length of time slice	5 s
Routing	
Vehicles communication range	500 m
Drones communication range	600 m
Drones altitude	200 m
Mac protocol	802.11p
Routing protocol	AODV [31]
% of nodes requesting data	10%
Radio-propagation model	TwoRayGround
Type of Traffic	Constant Bit Rate (CBR)
CBR Interval	0.1 s
Packet Size	512 Bytes

B. Analyses of Network performance

1) Packet Delivery Ratio (PDR)

The *Packet Delivery Ratio* (*PDR*) is the percentage of successfully delivered packets. It is calculated by P_R/P, which P_R represents the number of data packets received by the destination node, and P is the number of data packets generated by the source node. This metric can be also replaced by Packet Loss Rate, which is always equal to '1-*PDR*' and evaluates network in the same aspect. We compare the *PDR* of different VANETs scheme with a various number of drones. The simulation also considers the vehicles density, which is divided into the sparse scenarios (100 vehicles) and the dense scenarios (200 vehicles). Fig. 8 demonstrates the average *PDR* of these scenarios.

As displayed in Fig. 8, our MNAD has the highest *PDR* in all scenarios. The fixed drones (FD) and cruising drones (CD) assisted VANET show similar performances, which are better than ND only in sparse-vehicle scenarios. For the dense-vehicle scenario, the *PDR* of each scheme becomes decrease. These losses are attributed to the poor scalability of routing protocol, i.e., the network quality tends to be worse with increased nodes. More nodes can lead to more opportunities for connectivity as

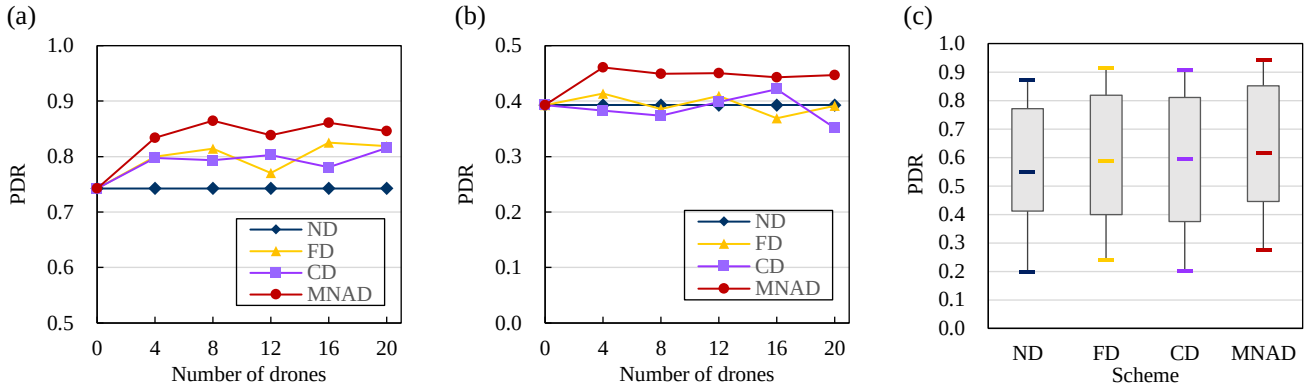

Fig. 8. (a) The average *PDR* of sparse-vehicle scenario. (b) The average *PDR* of dense-vehicle scenario. (c) Box-plot of *PDR* with 30 independent repeated experiments.

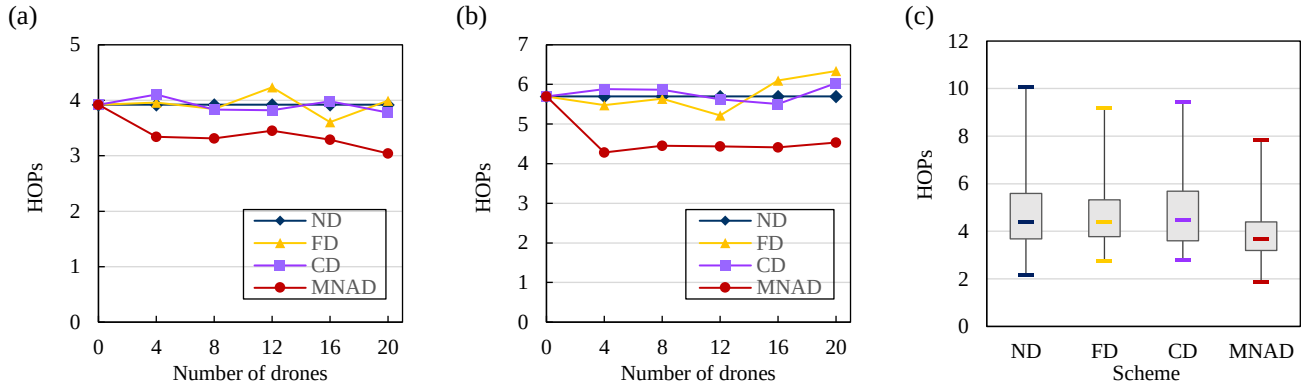

Fig. 9. (a) The *HOPs* of sparse-vehicle scenario. (b) The *HOPs* of dense-vehicle scenario. (c) Box-plot of *HOPs* with 30 independent repeated experiments.

well as more interference, load, computation, and changes. All these additions may result in potential accidents for routing protocol so that the scalability problem is unavoidable for any protocol. Under the common deterioration in the dense-vehicle scenario, MNAD still outperforms its contrast schemes with varies numbers of drones.

Due to the imbalance distribution and frequent movement of vehicles, the isolated node also appears with a sufficient number of vehicles. However, the probability will decrease with the growing number of vehicles, which has been verified by the changes of *PDR*. With consideration of isolated vehicles, the *PDR* improvement of our scheme for sparse scenario is about 10% while for dense scenario is only around 5%. Meanwhile, no improvement for other drone-assisted schemes in dense scenario. It means that the disconnected island rarely appears in dense scenario.

To observe the distribution of the results of the experiments, the box-plot *PDR* figure is presented by Fig. 8(c). It shows that all the indicators of box-plot of our proposed MNAD are higher than its contrasts. The highest *PDR* of MNAD has achieved 94%, which is superior to other schemes' upper limits. For the worst conditions, ND and CD are inefficient as lower than 20%, FD gets 23% but still no more than MNAD's 27%. Half of the MNAD's *PDR* is higher than 60%, which has a slight advantage to the other three schemes. For all metrics of the *PDR* boxplot, MNAD has noticeable superiorities to other schemes. Thus, it is considered to have higher PDR in general.

2) The average number of hops (HOPs)

The *HOPs* demonstrates the number of MAC layer transmissions made from source node to destination node. In other words, the number of hops is equal to the number of intermedia nodes on the communication path plus 1 (source node). More hops represent high cost on transmission link, i.e., an ideal link should have as few hops as possible. The statistical results of the *HOPs* are shown in Fig. 9.

There is no critical distinction of *HOPs* for ND, FD, and CD whatever the densities of vehicles and drones are. The only discrepancy is the unstable FD has relatively noticeable fluctuation. While for the MNAD, *HOPs* has been reduced in each scenario. With the sparse-vehicle scenario (100 vehicles in the simulation area), MNAD has about one hop advantage over other schemes. This advantage tends to grow with the increasing number of drones. In the dense-vehicle scenario, MNAD has almost two hops reduction than other comparison schemes which fluctuate around six hops. It is noticed that the *HOPs* are growing when the vehicles become dense.

As shown in box-plot Fig. 9(c), MNAD still has great superiority on all evaluation indictors. Three-quarters results of MNAD are lower than five hops, and the minimum is even less than two hops. For the worst hops, MNDA has clear two hops advantage to its competitors. The rational scheduling of drones

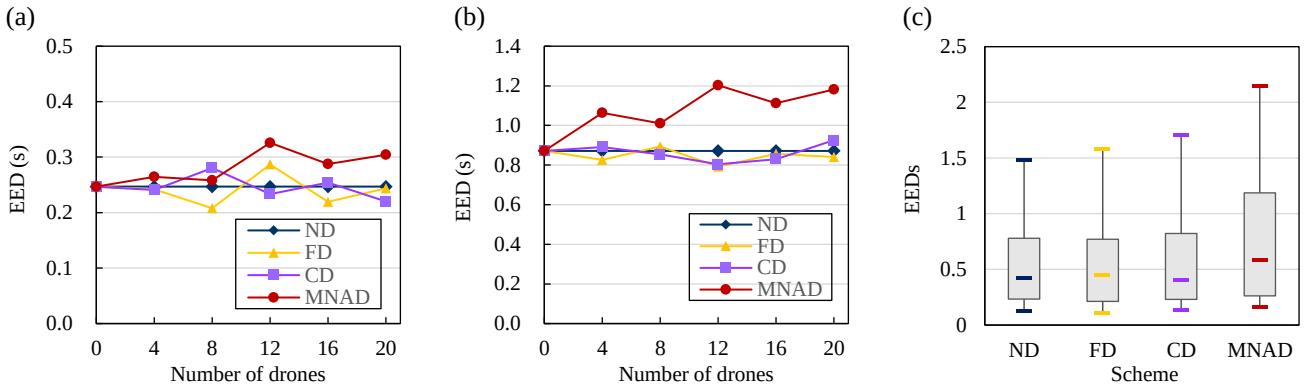

Fig. 10. (a) The average *EED* of sparse-vehicle scenario. (b) The average *EED* of dense-vehicle scenario. (c) Box-plot of average *EED* with 30 independent repeated experiments.

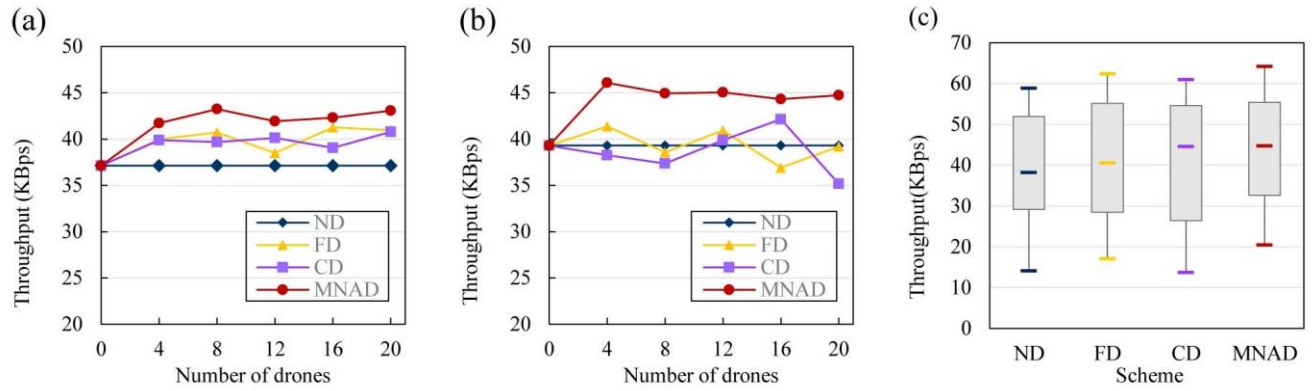

Fig. 11. (a) The *throughput* of sparse-vehicle scenario. (b) The *throughput* of dense-vehicle scenario. (c) Box-plot of *throughput* with 30 independent repeated experiments.

by our model and algorithm explains this advance. The existence of drones on the appropriate area can help the transmission avoid unnecessary hops. In contrast, the unplanned drones only play as redundant nodes and take the extra burden to the reactive routing protocol.

3) Average End-to-end Delay (EED)

End-to-end delay is the actual time taken by the transmission of a valid data packet. The average *EED* depends on the ratio of the total time taken (sum of each *EED*) to the number of successfully received packets. The network quality is evaluated by average *EED*, which is expected to be lower.

According to Fig. 10, drone-assisted mechanisms do not take effect in this metric. The average *EED* are arbitrarily fluctuating in the sparse-vehicle scenario. This condition also happens in dense-vehicle scenario expect for MNAD, which unfolds a worse tendency. That is due to the *EED*, as the real-time consumption of transmission, also includes the time of routing discovery. In urban VANET, because of the extremely high dynamic of vehicles, the routing discovery can be highly frequent. In this case, the time consumption of discovery cannot be neglected. It also should be noticed that the failed transmission is not considered in the computation of *EED*. Without our MNAD, the isolated vehicles are often in a state in which there will be no available routing path to the destination. These failed processes of routing discovery can contribute to the packet losses and additional time cost but with no impact for *EED*. For these complex scenarios, our scheme spends extra time on discovery but obtains a reachable path that improves the average result of *EED*.

As box-plot depicted in Fig. 10(c), there are at least half of the *EEDs* of MNAD beyond 0.5 second, which is worse than most of the other methods. More than one-quarters *EEDs* of MNDA are beyond 1 second; especially the maximum is reached 2.1 seconds. However, in comparison, even under the worst scenarios, the other three schemes are lower than 1.8 seconds. Due to our proposal expending extra time to obtain better accuracy on routing, this compromise between time consumption and accuracy results in that MNAD fail into disadvantage on *EEDs*. However, these defects can be overcome by geography-based routing protocols [6] whose time taken by path discovery is generally enough to be ignored.

4) Throughput

Throughput represents the total amount of data can be successfully transmitted during a period. This evaluation metric reflects the real transmission efficiency of the network. Fig. 11 gives the statistics of each scenario's throughput. Due to the application of the *Constant Bit Rate (CBR)* for routing traffic,

throughput is positively correlated with *PDR*. The statistics of *throughput* in Fig. 11 are similar to *PDR* in Fig. 8.

MNAD achieves the highest throughput among the four schemes. Although all the throughput is decreased in the dense-vehicle scenario, MNAD still keeps the highest performance. By reviewing the previous analysis of *PDR*, we would like to explain why MNAD achieves the best throughput despite its inferior *EED*. The calculation of *EED* only considers the successfully received packet, whereas quite a few packets are lost. Although other three schemes have lower average delay for each packet transmission, their heavy loss of packet results in fewer data transmitted during the same period, i.e., lower throughputs.

C. Summary of Simulation

Refer to the real maps and floating car data of Chengdu city in China, we design a series of simulations to exam the effectiveness and flexibility of our proposed MNA-optimized Drone-assisted (MNAD) VANET. The weakness of contrastive cases (ND, FD, and CD) verifies that the improvement of VANET which is due to the utilization of our proposed evaluation model and optimization algorithm rather than the simple adoption of drones. It can be seen that MNAD has outstanding performance in terms of *packet delivery ratio* (*PDR*), *average number of hops* (*HOPs*), and *throughput*. Increased *PDR* and *throughput* represent few-failed routing and high-quality links. In contrast, decreased *HOPs* means the shorter path. These improvements are benefited from the optimal distribution of multiple drones which are deployed at the most critical positions.

Another evaluation metric *average end-to-end delay* (*EED*) gets a little loss with MNAD that is attributed to the compromise between routing discovery time and routing quality. However, the improvements in *throughput* have rectified that this compromise is worthwhile. For the global perspective, higher throughput represents the MNAD mechanism could transmit more valid packets with the same duration.

For the number of drones, diverse simulations have illustrated that the increasing number of drones is unnecessary. A limited number of drones, such as 8 drones in 2 km × 2 km area, are sufficient for assisting VANET with noticeable improvement while more drones take no advantage or even some negative effect. In other words, the scalability problem also emerges in our scheme. Nevertheless, it has few impacts because our scheme is proposed specifically for infrastructure-less scenarios. This paper intends to fill the shortage of network infrastructure, in which the communication model is equipped on the dynamic drones to receive the intelligent dispatching schedules. If there were more drones act as relay nodes to guarantee the full coverage, a schedule will not be necessary, an issue that is out of the scope of this paper.

V. Conclusion

In this work, we designed a collaborative-based drone-assisted VANET networking model. In this model, FANET consists of drones that serve as relay nodes in the air. The deployment of drones relies on the prediction of vehicles distribution, which helps isolated vehicles routing, NLoS, and load balancing networking. To enable better collaboration of multiple drones, the best distribution of drones is transferred into a multimodal optimization problem. In particular, we propose a novel intelligent multimodal algorithm, named Multimodal Nomad Algorithm, to solve the problem efficiently. According to the number of drones, this algorithm can obtain multiple optimal positions for drones simultaneously. Simulation experiments have been conducted to test network performance. We compared our model with conventional VANET, VANET with fixed auxiliary drones, and cruising drones assisted VANET without optimization. The experimental results demonstrate that our proposed Multimodal Nomad Algorithm optimized Drone-assisted VANET is superior to other models in terms of average packet delivery rate, the average number of hops (*HOPs*), and throughput. Although the end-to-end delay of our proposal has a slight loss, the increase in throughput has verified the global transmission capability is improved. In urban VANETs, our collaborative networking model is promising for large-scale data transmission application, such as onboard multimedia transmission. As a concrete step towards future work, integrating our proposed model with other networks, such as the software-defined network, can enhance the management and network control.

Acknowledgment

This study is funded by the Key Projects of Liaoning Provincial Department of Education Science Foundation (L201702), the National Science Foundation of China (61701322), the Young and Middle-aged Science and Technology Innovation Talent Support Plan of Shenyang (RC190026) and the Liaoning Provincial Department of Education Science Foundation (JYT19052).

References

[1] B. Hassanabadi and S. Valaee, "Reliable periodic safety message broadcasting in VANETs using network coding," *IEEE Trans. Wireless Commun*., vol. 13, no. 3, pp. 1284-1297, Mar. 2014.

[2] J. Chen, G. Mao, C. Li, W. Liang, and D. Zhang, "Capacity of cooperative vehicular networks with infrastructure support: Multiuser case," *IEEE Trans. Veh. Technol*., vol. 67, no. 2, pp. 1546-1560, Feb. 2018.

[3] N. Lu, N. Cheng, N. Zhang, X. Shen, and J. W. Mark, "Connected vehicles: solutions and challenges," *IEEE Internet of Things J*., vol. 1, no. 4, pp. 289-99, Aug. 2014.

[4] M. Sivasakthi and S. R. Suresh, "Research on vehicular ad hoc networks (VANETs): an overview," *Int. J. Appl. Sci. Eng. Res*., vol. 2, no.1, pp. 23-27, Sep. 2013.

[5] J. Cheng, J. Cheng, M. Zhou, F. Liu, S. Gao, and C. Liu, "Routing in internet of vehicles: A review," *IEEE Trans. Intell. Transp. Syst*., vol. 16, no. 5, pp. 2339-2352, Oct. 2015.

[6] S. Boussoufa-Lahlah, F. Semchedine, L. Bouallouche-Medjkoune, "Geographic routing protocols for Vehicular Ad hoc NETworks (VANETs): A survey," Veh. Commu., vol. 11, pp. 20-31, Jan. 2018.

[7] C. Campolo and A. Molinaro, "Multichannel communications in vehicular ad hoc networks: A survey," *IEEE Commun. Mag.*, vol. 51, no. 5, pp. 158-169, May. 2013.
[8] R. Molina-Masegosa and J. Gozalvez, "LTE-V for sidelink 5G V2X vehicular communications: A new 5G technology for short-range vehicle-to-everything Communications," *IEEE Veh. Technol. Mag.*, vol. 12, no. 4, pp. 30-39, Dec. 2017.
[9] W. Shi, H. Zhou, J. Li, W. Xu, and N. Zhang, "Drone assisted vehicular networks: architecture, challenges and opportunities," *IEEE Netw.*, vol. 32, no. 3, pp. 130-137, May/Jun. 2018.
[10] I. Bekmezci, O. K. Sahingoz, and S. Temel, "Flying ad-hoc networks (FANETs): A Survey," *Ad Hoc Netw.*, vol. 11, no. 3, pp. 1254-1270, May. 2013.
[11] J. Wu, L. Zou, L. Zhao, A. Al-Dubai, L. Mackenzie, and G. Min, "A Multi-UAV Clustering Strategy for Reducing Insecure Communication Range," Comput Netw., vol. 158, pp. 132-142, Jul. 2019.
[12] C. Luo, W. Miao, H. Ullah, S. McClean, G. Parr, and G. Min "Unmanned Aerial Vehicles for Disaster Management, in Springer Natural Hazards, Geological Disaster Monitoring Based on Sensor Networks., T. S. Durrani, W. Wang, and S. M. Forbes, Eds., Singapore: Springer Singapore, 2019, pp. 83107.
[13] Unmanned aircraft systems: Air-ground channel characterization for future applications," IEEE Vehicular Technology Magazine, vol. 10, no. 2, pp. 79–85, 2015.
[14] UAV-assisted supporting services connectivity in urban VANETs. IEEE Transactions on Vehicular Technology, 2019, vol. 68, no 4, p. 3944-3951.
[15] C. Sommer, D. Eckhoff, R. German, F. Dressler, "A computationally inexpensive empirical model of IEEE 802.11p radio shadowing in urban environments," *Proc. 2011 8th Int. Conf. Wireless On-Demand Netw. Syst. Serv.*, pp. 84-90, 2011.
[16] Leveraging Communicating UAVs for Emergency Vehicle Guidance in Urban Areas. IEEE Transactions on Emerging Topics in Computing, 2019.
[17] X. Wang, L. Fu, Y. Zhang, X. Gan, and X. Wang, "VDNet: An infrastructure-less UAV-assisted sparse VANET system with vehicle location prediction," *Wireless Commun. Mobile Comput.*, vol. 16, no. 17, pp. 2991-3003, Sep. 2016.
[18] O. S. Oubbati, A. Lakas, M. G¨unes¸, F. Zhou, and M. B. Yagoubi, "UAV assisted reactive routing for urban VANETs," in Proc. Symp. Appl. Comput.,ACM, 2017, pp. 651–653
[19] H. Seliem, R. Shahidi, M. H. Ahmed, and M. S. Shehata, "Drone-based highway-VANET and DAS service," *IEEE Access.*, vol. 6, pp. 20125-20137, 2018.
[20] O. S. Oubbati, A. Lakas, F, Zhou, M. Gunes, N. Lagraaet, and M. B. Yagoubi, "Intelligent UAV-assisted routing protocol for urban VANETs," *Computer Communications*., vol. 107, pp. 93-111, July. 2017.
[21] N. Zhang, S. Zhang, P. Yang, O. Alhussein, W. Zhuang, and X. Shen, "Software defined space-air-ground Integrated vehicular networks: challenges and solutions," *IEEE Commun. Mag.*, vol. 55, pp. 101-109, Mar. 2017.
[22] X. Li, M. G. Epitropakis, K. Deb, and A. Engelbrecht, "Seeking multiple solutions: An updated survey on niching methods and their applications," *IEEE Trans. Evol. Comput.*, vol. 21, no. 4, pp. 518-538, Aug. 2017.
[23] J. Liang, B. Qu, X. Mao, and T Chen, "Differential evolution based on fitness Euclidean-distance ratio for multimodal optimization," *Neurocomputing*., vol. 137, pp. 252-260, Aug. 2014
[24] C. Rim, S. Piao, G. Li, and U. Pak, "A niching chaos optimization algorithm for multimodal optimization," *Soft Comput*., vol. 22, no. 2, pp. 621-633, Jan. 2016.
[25] Q. Yang, W. Chen, Z. Yu, T. Gu, Y. Li, H. Zhang, and J. Zhang, "Adaptive Multimodal Continuous Ant Colony Optimization," *IEEE Trans. Evol. Comput*., vol. 21, no. 2, pp. 191-205, Apr. 2017.
[26] N. Nekouie and M. Yaghoobi, "A new method in multimodal optimization based on firefly algorithm," *Artif Intell Rev*., vol. 46, no. 2, pp. 267-287, Aug. 2016.
[27] B. Y. Qu, P. N. Suganthan, and J. J. Liang, "Differential evolution with neighborhood mutation for multimodal optimization," *IEEE Trans. Evol. Comput.*, vol. 16, no. 5, pp. 601-614, Oct. 2012.
[28] J. Li and Y Tan, "Loser-Out Tournament-Based Fireworks Algorithm for Multimodal Function Optimization," *IEEE Trans. Evol. Comput.*, vol. 22, no. 5, pp. 679-691, Oct. 2018.
[29] J. Kennedy and R. Eberhart, "Particle swarm optimization," in *Proceedings of ICNN'95-International Conference on Neural Networks*., Perth, WA, Australia, Nov. 1995, pp. 1942–1948.
[30] E. Rashedi, H. Nezamabadi-Pour, and S. Saryazdi, "GSA: a gravitational search algorithm," Inf Sci., vol. 179, no. 13, pp. 2232-2248, Jun. 2009.
[31] X. S. Yang, M. Karamanoglu, and X. He, "Flower pollination algorithm: a novel approach for multi objective optimization," *Engineering Optimization*., vol. 46, no. 9, pp. 1222-1237, Sep. 2014.
[32] S. Mirjalili and A. Lewis, "The whale optimization algorithm," Adv Eng Softw., vol. 95, pp. 51-67, May. 2016.
[33] A. Askarzadeh, "A novel metaheuristic method for solving constrained engineering optimization problems: crow search algorithm," *Comput Struct*., vol. 169, pp. 1-12, 2016.
[34] J. W. Pepper, B. L. Golden, and E. A. Wasil, "Solving the traveling salesman problem with annealing-based heuristics: A computational study," *IEEE Trans. Syst. Man Cybern. A Syst. Humans*, vol. 32, no. 1, pp. 72-77, Jan. 2002.
[35] A 3D Smooth Random Walk Mobility Model for FANETs. 21th IEEE HPCC-2019, pp. 460-467.
[36] K. Fall, K. Varadhan. [2007]. The Network Simulator (ns-2). [Online]. Avaliable: http://www.isi.edu/ nsnam/ns.
[37] C. E. Perkins, E. M. Royer, and S. Das, *Ad Hoc On-Demand Distance Vector (AODV) routing*, 2003, [online] Available: http://www.ietf.org/rfc/rfc3561.txt.
[38] OpenStreetMap. [Online]. Avaliable: http://www.openstreetmap.org/.
[39] Didi Chuxing GAIA Initiative. [Online]. Avaliable: https://gaia.didichuxing.com
[40] D. Krajzewicz, J. Erdmann, M. Behrisch, and L. Bieker, "Recent development and applications of SUMO—Simulation of urban mobility," *Int. J. Adv. Syst. Meas.*, vol. 5, no. 3/4, pp. 128-138, 2012.